Mar Biotechnol (2009) 11:62–73
DOI 10.1007/s10126-008-9120-y

ORIGINAL ARTICLE

A New Prokaryotic Farnesyldiphosphate Synthase from the Octocoral *Eunicea Fusca*: Differential Display, Inverse PCR, Cloning, and Characterization

Llanie K. Ranzer · Thomas B. Brück · Wolfram M. Brück · Jose V. Lopez · Russell G. Kerr

Received: 10 January 2008 / Accepted: 3 June 2008 / Published online: 15 July 2008

Abstract We recently reported that the biosynthesis of fuscol, a diterpene from the octocoral *Eunicea fusca*, is inducible by the application of plant signaling factors such as salicylic acid to the coral's algal symbiont. In this study, an mRNA differential display approach has been employed with the dinoflagellate symbiont of this octocoral which has led to the isolation of a farnesyldiphosphate synthase (FPPS) that was transcriptionally activated under conditions that led to an induction of fuscol biosynthesis. Using a degenerate primer based on the aspartate-rich motifs found in prenylsynthases and a cassette ligation strategy, we report the cloning of the complete FPPS associated with the *E. fusca* dinoflagellate symbiont *Symbiodinium* sp. The protein exhibited the enzymatic properties associated with FPPS, namely, the synthesis of farnesyl diphosphate from geranyldiphosphate and isopentenyl diphosphate. The amino acid sequence of this FPPS has a high sequence similarity (82%) to known archaeal isoprenyl diphosphate synthases. This is the first description of a prokaryotic FPPS derived from a marine source.

Keywords Fuscol · Farnesyl diphosphate synthase · Differential display · IPCR · Characterization · Gorgonian

L. K. Ranzer · T. B. Brück · R. G. Kerr
Center of Excellence in Biomedical and Marine Biotechnology,
Department of Chemistry and Biochemistry,
Florida Atlantic University,
777 Glades Rd.,
Boca Raton, FL 33431, USA

W. M. Brück
Centre of Applied Marine Biotechnology,
Letterkenny Institute of Technology,
Port Road,
Letterkenny, County Donegal, Republic of Ireland

J. V. Lopez
Nova Southeastern University,
Dania Beach, FL 33004, USA

R. G. Kerr (✉)
Department of Chemistry and Department of Biomedical Sciences,
University of Prince Edward Island,
550 University Drive,
Charlottetown, PEI C1A 4P3, Canada
e-mail: rkerr@upei.ca

Introduction

Terpenes represent the largest class of natural products and are of interest due to their biological activity in areas of relevance to human health and chemical ecology. We have had a long-standing interest in the biosynthesis of terpenes of marine origin and recently reported that terpene biosynthesis is inducible in a dinoflagellate preparation of a gorgonian coral (Newberger et al. 2006). While little is known about terpene biosynthesis in marine systems, significant progress has been made with plants of terrestrial origin. Notably, the inducibility of terpene biosynthesis has been reported in a variety of plants. For instance, salicylic acid (SA) and methyl jasmonate (MeJA) stimulate a prophylactic defense and resistance mechanism via terpenoids in uninfested plants during insect wounding on neighboring plants (Shulaev et al. 1997). MeJA has also been shown to upregulate terpene biosynthesis in the leaves of *Vitis vinifera* (Sembdner and Parthier 1993; Hampel et al. 2005). There are also reports of the cloning and expression of terpene biosynthetic genes from induction experiments in plants (e.g., Bohlmann et al. 1998).

The goal of the work described herein was to use previously developed conditions (Newberger et al. 2006) to induce terpene biosynthesis in a marine system while utilizing the mRNA differential display (DD; Laing and Pardee 1992) approach to identify one or more genes involved in terpene production. This method allows for the identification of differentially expressed genes by nonstringent reverse transcriptase polymerase chain reaction (RT-PCR) with different sets of 3′-anchored RT primers and additional upstream PCR primers. As previously reported, terpene biosynthesis can be induced in a dinoflagellate preparation of the coral *Eunicea fusca*. Specifically, the production of the predominant terpene isolated from this coral, fuscol, was upregulated in response to treatment with methyl jasmonate, salicylic acid, and gibberellic acid.

Prenyl synthases are key terpene biosynthetic genes and function at the branch points of isoprenoid metabolism and are considered to play a regulatory role in controlling the flux distribution of isopentenyl diphosphate (IPP) into the various terpenoid families (Gershenzon and Croteau 1993). Comparison of amino acid sequences of prenyl synthases from various organisms reveals the presence of several highly conserved regions (Koyama et al. 1993; Chen et al. 1994). These conserved regions can serve as templates for degenerate PCR primer design. Thus, prenyl synthases represent a rationale target for this DD approach with the coral *E. fusca*.

Materials and Methods

Dinoflagellate Isolation and Induction

E. fusca samples were collected off Long Key, in the Florida Keys during January of 2004 by SCUBA. Coral tissue (typically 30 g) was homogenized in a Waring blender using 100 ml deionized water, and the homogenate filtered through cheesecloth. The *Symbiodinium* sp. cells were pelleted by centrifugation at 900×*g* and washed ten times with 45 ml of 0.2 μ filtered seawater (FSW). The algal symbionts were further purified by a discontinuous Percoll™ gradient twice. The cells were then rinsed with FSW twice, resuspended in FSW, and then counted by hemocytometer using light microscopy. Dinoflagellates were allowed to equilibrate in BD Falcon T-flasks™ for 24 h before treatment. Three replicates of 2.0×10^7 cells were used for each of the following treatments and a control: 50 μM SA, 100 μM SA, 200 μM SA, and 300 μM SA. The dinoflagellates were maintained for 48 h and then fuscol isolated and quantified as we have previously described (Newberger et al. 2006).

RNA Extraction and mRNA Differential Display Analysis

Total RNA was isolated from the induced *Symbiodinium* sp. cultures using the RNeasy Mini Kit (Qiagen) by grinding recommended amounts of tissue (1×10^7 cells per mini-column) with liquid nitrogen (LN_2) in a frozen mortar and pestle taking care not to let the tissue thaw until placed in the appropriate lysis buffer supplied with the kit. Possible DNA contamination was removed by on-column DNase digestion with the RNase-Free DNase set. RNA was then eluted twice in a total volume of 50 μl of RNase-free H_2O. The two elutions were combined and precipitated with GlycoBlue (Ambion). RNA was quantified by measuring A_{260} absorbance in a Molecular Devices Spectra Max Plus plate-reader. Purity was assessed by calculating the A_{260}/A_{280} ratio. Samples were immediately aliquoted (0.1 μg/μl) and stored at −80°C. Samples were loaded (0.5–1.0 μg of RNA) in a 1.2% agarose gel, run at 100 V for 1.5 h, and stained with ethidium bromide. Gels were visualized using a Typhoon 9410 variable mode imager (GE LifeSciences).

Differential display was performed using RNAimage Kit (GenHunter) according to the manufacturer's instructions with some minor exceptions. Total RNA (200 ng) from the control and each of the 50, 100, 200, and 300 μM SA treatments were reverse transcribed with "xscript"-reverse transcriptase (Promega) in the presence of 2 μM H-T_{11}A as the anchored primer. Two microliters of the reaction was then used for PCR. The anchored primer H-T_{11}A included in the kit and the GGPS-2S primer (Takaya et al. 2003; Table 1) were used during the PCR step. This primer was chosen in order to obtain predominantly prenyl diphosphate-related PCR products with this DD method. PCR products

Table 1 List of primers with target sequences

Primer name	Primer sequence	Use
GGPS-2S	ATGWSIYTIATHCAYGAYGA	Differential display
EFZ265F	GGATTGCTTGTTGCTCTTGA	Reamplification of EST
EFZ265RC	CTCCAACCGATAAAGCTCCA	Reamplification of EST
Sau265S13′	AACAAGAAAAATTAAAGAGATTTGGAGAAT	IPCR/SP-PCR
Sau265S23′	AAGAAAAATTAAAGAGATTTGGAGAATG	IPCR/SP-PCR (nested)
Sau265S25′	AACAAGCAATCCTTTTGAAGTAAATAAT	IPCR/SP-PCR
Sau265S35′	TTTGAAAGTAAATAATCGCCAACTAAAACT	IPCR/SP-PCR (nested)
265 forward	ATGAGTTTGAAAAAAAGTAGTATTAGTATTATTAAAGC	Gene expression
265 reverse	TTTTGTTCTCGAGATGGTGTATTCT	Gene expression

were analyzed on gels cast with Gene-Gel 6% (BioShop Canada). Gels were dried on a Hoefer SE 1160 Drygel Sr. (GE LifeSciences) and radiographic films were aligned to the gels and exposed for 48 h. A Kodak X-OMAT was used to develop the films. The reproducibility of the DD analysis was confirmed by repeating the experiments in multiple reaction lanes. mRNA transcripts corresponding to the trend found in the induction of fuscol with SA were chosen for further examination. Differentially expressed cDNA fragments were eluted from the sequencing gel, ethanol precipitated, and reamplified using the same primer set. Reamplified DNA was analyzed on agarose gels, and bands of expected size (~450 bp) were purified and subsequently cloned into the plasmid vector.

Cloning and Sequence Analysis

PCR products were cloned with a TOPO TA cloning kit according to the manufacturer's instructions (Invitrogen). The cloned PCR products were sequenced using the Big Dye Terminator v3.1 Cycle Sequencing Kit (Applied Biosystems), on an ABI 3100 automated sequencer (Applied Biosystems).

DNA Extraction, Inverse PCR, and Single Primer PCR

Genomic DNA (gDNA) was extracted from the induced cells using GNOME (BIO 101) according to the manufacturer's protocol. Two individual pools (*Xba I* and *Pst I* digested) of cassette-ligated gDNA fragments were constructed according to the manufacturer's instructions. These two pools were then used as libraries to isolate the genome-specific sequences of the EFZ265 fragment by PCR-based genome walking method (TaKaRa, LA PCR in vitro Cloning Kit). Primers used in this study are listed in Table 1.

First round PCR for the single-primer PCR reaction consisted of 2 μl of LA-Taq, 5 μl of 10× LA Buffer, 8 μl of 10 μM deoxyribonucleotide triphosphates (DNTPs), 2 μl of the a single primer (10 μM), 32 μl water, and 1 μl of digested gDNA (10 ng). PCR conditions were 98°C for 3 min, 35 cycles of 95°C for 60 s, 60°C for 30 s, and 72°C for 60 s, followed by 10 min of elongation at 72°C. An aliquot of the first round PCR reaction was diluted 1:10 and 3 μl was reamplified using the conditions described above, adjusting the amount of water accordingly, and using the appropriate (3′ or 5′) nested primer. By comparing and assembling the core fragment, 3′ and 5′ inverse PCR products, the isolate, EFZ265, was deduced.

Nucleotide Sequence Accession Number

The nucleotide sequence data reported herein have been submitted to the GenBank database under accession number EF011562.

Bioinformatics and Phylogeny Analysis

For the identification of functional homologues, the nucleotide and translated protein sequence obtained in this study was compared to other nucleotide/amino acid sequences using National Center of Biotechnology Information (NCBI) Basic Local Alignment Search Tool (BLAST)X [http://www.ncbi.nlm.nih.gov/BLAST/] (Altschul et al. 1997; Schäffer et al. 2001). For a more detailed protein classification and the identification of catalytic domains, the protein sequence was analyzed using the domain architecture analysis tool (DART) [http://www.ncbi.nlm.nih.gov/Structure/lexington/lexington.cgi?cmd=rps] (Geer et al. 2002) in conjunction with NCBI's conserved domain database (CDD) [http://www.ncbi.nlm.nih.gov/Structure/cdd/wrpsb.cgi] (Marchler-Bauer et al. 2005).

For phylogenetic analysis of the translated protein sequence obtained in this study, sequences of archaeal, bacterial, and eukaryotic isoprenyl diphosphate synthases were either directly retrieved from BLAST results or from NCBI's Protein sequence repository (http://www.ncbi.nlm.nih.gov/sites/entrez?db=Protein). Amino acid sequence alignments were made with CLUSTAL X version 1.83 (Thompson et al. 1997). Multiple alignment parameters were used as follows: gap opening penalty, 15; gap extension penalty, 0.3; delay divergent sequences, 25%. Alignments were manually checked and are available from the authors upon request. Neighbor-joining distance analysis of the aligned sequences were conducted using phylogenetic analysis using parsimony for windows version 4.0 beta (Swofforf 2001). To determine the strength of each internal node, a bootstrap analysis was conducted with a heuristic algorithm and 1,000 replications.

Functional Expression of the Recombinant Protein

Vent DNA Polymerase (New England BioLabs) was used to obtain the open reading frame (ORF) containing blunt ends using the gene expression primers listed in Table 1. The PCR reaction consisted of 2 μl of 10 mM DNTPs, 3 μl of each primer (10 μM), 10 ng of gDNA isolated from induced cells, 4 μl of 25 mM $MgSO_4$, 10 μl of 10× buffer, 0.5 μl of *Vent* DNA polymerase, and 76.5 μl of nuclease-free water. PCR conditions were 95°C for 4 min, 30 cycles of 95°C for 30 s, 50°C for 30 s, 72°C for 70 s, followed by 7 min of elongation at 72°C. Quantum Prep Freeze 'N Squeeze DNA Gel Extraction Spin columns (Bio-Rad) was used to gel purify the amplicon which was then ethanol-precipitated. One microliter of the ethanol-precipitated sample was reamplified using Platinum *Pfx* master mix (Invitrogen) with the following PCR conditions: 95°C for 5 min, 25 cycles of 95°C for 30 s, 50°C for 30 s, 68°C for 70 s, followed by 7 min of elongation at 68°C.

Champion pET Directional TOPO Expression Kit (Invitrogen) was used to clone and express the reamplified blunt-ended full gene product according to the manufacturer's instructions. Isopropyl-beta-D-thiogalactopyranoside (IPTG) of 1 mM was used to induce the cultures for 5 h (optical density $(OD)_{600}$=~2.0). The uninduced and induced cultures were harvested by centrifugation (27.000 *g*/15 min) and stored at −80°C. A 1.5 ml of incubation buffer (50 mM potassium phosphate, pH 7.2, 10 mM dithiothreitol (DTT), 10 mM $MgCl_2$, 0.5 mM $CaCl_2$, 1 mM phenylmethylsulphonyl fluoride (PMSF), 0.25 mg/ml bovine serum albumin) was added to these pellets. The cell suspension was thoroughly sonicated on ice and 500 µl of the sonicated samples were used for the enzyme-catalyzed reactions.

Protein concentrations were assessed using the Bradford method (Bradford 1976). The presence of the recombinant protein was assessed by sodium dodecyl sulfate polyacrylamide gel electrophoresis (SDS-PAGE) using the NUPAGE™ (8*8 cm, 4–12% T linear gradient) ready-gel system according to manufacturer protocols (Invitrogen). Proteins were subsequently visualized by Coomassie R-250 staining according to standard protocols (Lammlie 1970).

Enzyme Activity Assays and HPLC Product Analysis

The reaction mixture containing 0.4 mM IPP, 10 µg of *E. fusca* farnesyl diphosphate (FPP) synthase (in the 500 µl of sonicated cell homogenate) together with 0.4 mM of either unlabeled dimethylallyl pyrophosphate (DMAPP), geranyldiphosphate (GPP), or FPP was incubated in 500 µl buffer (50 mM potassium phosphate, pH 7.2, 10 mM DTT, 10 mM, $MgCl_2$, 1 mM PMSF, 0.5 mM $CaCl_2$) for 2 h at 34°C. Reactions were quenched with 20 µl of 100 mM ethylenediaminetetraacetic acid (EDTA), pelleted, and the supernatant analyzed by reversed phase-high performance liquid chromatography (RP-HPLC).

Analytical-scale chromatography was performed on a Perkin Elmer LC-235 HPLC unit equipped with ultraviolet–visible spectroscopy diode array detector. NH_4HCO_3 of 25 mM, pH 8.0, was used to dissolve samples and as the aqueous component in reverse-phase HPLC. Sample elution was achieved by using a linear (95% to 5% *v*/*v*) H_2O to acetonitrile gradient at a flow rate of 1 ml/min. Preparative-scale separations were on a 250×22-mm Vydac C18 column (Zhang and Poulter 1993). Prior to sample analysis, elution windows for possible isoprenyl synthase reaction products were determined by individually measuring the retention times for 10 µg GPP, geraniol (GOH), FPP, farnesol (FOH), geranylgeranyl diphosphate (GGPP), and geranylgeraniol (GGOH). During sample analysis, GPP (10 µg), FPP (10 µg), and GGPP (25 µg) were co-injected and used as standards.

Ni-affinity Purification of the Recombinant Protein

The IPTG induced *Escherichia coli* cultures were harvested by centrifugation at 27,000 *g* for 15 min. Pellets were resuspended in 3 ml of isolation buffer (50 mM 3-(*N*-morpholino)propanesulfonic acid, pH 8, 10 mM DTT, 10 mM $MgCl_2$, 0.5 mM $CaCl_2$, 1 mM PMSF, 5% (*v*/*v*) Tween 20, 0.25% (*v*/*v*) Triton X-100) and sonicated on ice for 3 min. The resulting slurry was centrifuged at 50,000 *g* (4°C) and the cleared supernatant (1.32 ml) was loaded on a HisTrapFF Ni-affinity (5 ml bed volume, GE LifeSciences) column that was pre-equilibrated with seven column volumes of isolation buffer for purification on an Äkta Purifier 10 fast protein liquid chromatography (FPLC) system (GE LifeSciences). Proteins were eluted with a gradient (1 ml/min) 0, 10, 25 and 200 mM imidiazole steps (12 min/step). The resin was then regenerated by using a 500 mM imidiazole wash for 5 min (1 ml/min) followed by equilibration with isolation buffer. The purification process was monitored by analyzing 1 ml fractions collected during the FPLC procedure by SDS-PAGE and enzyme activity measurements as described above. Purified enzyme factions were pooled and desalted with isolation buffer using an Amicon Ultrafiltration system (Millipore), equipped with a 10 kDa cutoff filter. One-milliliter aliquots of purified protein were stored at −80°C.

Determination of Enzyme Specificity Using DMAPP, GPP, and FPP as Substrates

All kinetic reactions were conducted with Ni-affinity purified enzyme fractions. Substrate specificities of the putative isoprenyl diphosphate synthase were determined by using a combination of standard procedures reported in the literature (Ding et al. 1991; Wiedemann et al. 1993; Stanley-Fernandez et al. 2000; Dhiman et al. 2004). To determine the substrate specificity of the putative isoprenyl diphosphate synthase, a steady kinetic study was conducted with DMAPP, GPP, FPP, and IPP as substrates. Individual reactions were carried out in Eppendorf tubes in a total volume of 0.1 ml assay buffer (50 mM potassium phosphate, pH 7.2, 10 mM DTT, 5 mM orthovanadate, 15 mM $MgCl_2$, 0.2 mM $CaCl_2$, 1 mM PMSF, 2% (*v*/*v*) Tween20, 0.25% (*v*/*v*) Triton X-100) containing 10 µg (26.31 pmol) of soluble isoprenyl diphosphate synthase.

For the determination of rate constants of the allylic substrates DMAPP, GPP, and FPP, reaction mixtures contained variable concentrations (0–1,000 µM) of the respective unlabeled (cold) allylic isoprenyl diphosphate and a constant concentration of 80 µM [4-^{14}C]-labeled IPP (specific activity= 10 μC_i/µmol, GE LifeSciences) to enable detection of reaction products (Wiedemann et al. 1993; Dhiman et al. 2004). By contrast, the kinetic constants for the cosubstrate IPP were determined, by mixing variable amounts (0–200 µM) of

[4-^{14}C]-labeled IPP (specific activity=10 μC$_i$/μmol, GE LifeSciences) and 250 μM of unlabeled GPP (Dhiman et al. 2004).

All reactions were performed in triplicate by incubating at 37°C for 1 h and subsequently quenched by the addition of 100 mM EDTA. The radiolabeled isoprenyl diphosphate reaction products were extracted by solvent partitioning with 0.5 ml of 1-butanol (Ding et al. 1991). Samples were centrifuged at 50,000 *g* (4°C) for 2 min and the supernatant was removed. For rapid butanol removal, samples were further processed by refrigerated vacuum centrifugation. Subsequently, samples were resuspended in reaction buffer (50 mM Tris-HCl, 10 mM $MgCl_2$, pH 9) and incubated at 37°C for 2 h with 85 U of calf intestinal alkaline phosphatase (GE LifeSciences) to hydrolyze the prenyl diphosphate reaction products into their corresponding alcohols for analysis due to their increased stability (Stanley-Fernandez et al. 2000). Samples were again centrifuged at 10,000 *g* (4°C) for 2 min and the supernatants were immediately subjected to C18 RP-HPLC as described above. For the verification of the retention times, 10 μg of either unlabeled GOH, FOH, and GGOH was co-injected with each sample depending on the expected enzymatic reaction product. Fractions were collected at the elution windows previously determined for the reaction products geraniol (RT=17–20 min), farnesol (RT=23–25 min), and geranylgeraniol (RT=27–28 min). Solvent was rapidly removed using refrigerated vacuum centrifugation, followed by the addition of 10 ml scintillation fluid. The radioactivity of each sample was measured using an LKB scintillation counter (LKB-Bromma). Reaction velocities were determined from radioactivity counts and normalized relative to a blank reaction, which contained no protein. Reported activities are the mean of three activity measurements. Reactions were assayed under conditions in which product formation was linear for both time and protein concentration.

Kinetic constants (K_m, V_{max}, and k_{cat}) were determined by nonlinear fitting of the data to the Michaelis–Menton equation using the Slidewrite Plus graphics program (V5.01, Advanced Graphics Software).

Determination of Optimal Mg^{2+} Concentrations and pH for Catalysis

The optimal Mg^{2+} ion concentration (0–10 mM) for the isoprenyl diphosphate synthase reaction was determined using the reaction assay buffer mixture in the absence and presence of metal ion salts. The reaction mixtures also contained unlabeled GPP (200 μM) and 40 μM [4-^{14}C] labeled IPP (specific activity=10 μC$_i$/μmol, GE LifeSciences) to enable detection of product formation.

To determine the optimal pH of the reaction, the same assay setup as described for the Mg^{2+} dependent reactions was used except that the Mg^{2+} ion concentration was held constant at 15 mM and the pH of the assay buffer was varied between 5 and 10. For reactions above pH 7.5 we substituted the 50 mM phosphate buffer with a Tris-HCl buffer system of equivalent ionic strength due to the enhanced Tris-buffering capacity in the alkaline pH range. Procedures for reaction mixture incubation and sample processing were identical to those described for the kinetic studies with DMAPP, GPP and FPP.

Results

Differential Display

The differential display method was used to identify differences in mRNA levels following the addition of different concentrations of a known terpene inducer, salicylic acid (Fig. 1). The nucleotide sequences obtained from the excised bands were used as queries in BLASTX searches against protein databases. A 450-bp fragment, EFZ265, was found to resemble bacterial polyprenyl diphosphate synthases during a translated BLAST search (e-value=9×10^{-53}), and when compared to other prenyl diphosphate synthases, this clone was found to encode an internal portion of the gene containing both the first aspartate-rich motif (FARM) and the second aspartate-rich motif (SARM).

Isolation of Full-Length cDNA

Genomic DNA was isolated from a zooxanthellae preparation that had been treated for 24 h with SA in order to maximize the opportunity to isolate the full-length gene if expressed at low levels. The gDNA was then digested with *Xba I* or *Pst I* (data not shown) and ligated to the corresponding cassette for ligation-mediated PCR incorporating primers described in Table 1. Concurrently, single-

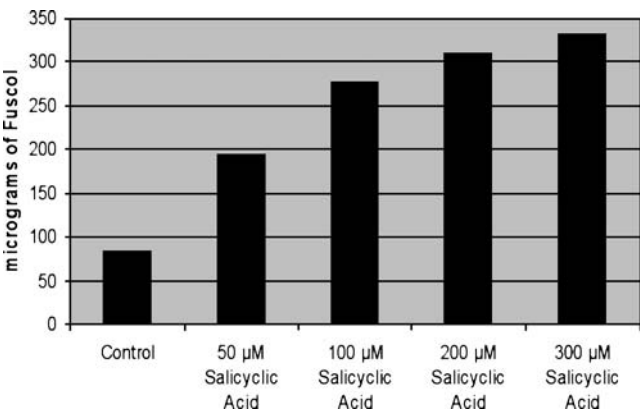

Fig. 1 Yields of fuscol from dinoflagellate cells treated with salicylic acid

primer PCR was used with the digested gDNA and the corresponding primers (Table 1) to obtain the upstream and downstream sequence of the EFZ265 fragment. Both methods led to the isolation of the full-length EFZ265 clone.

The ORF for the full-length prenyl diphosphate synthase gene encodes a protein of 328 amino acids, 984 nucleotides, with a calculated molecular mass of 38 kDa. The deduced protein is slightly basic with an isoelectric point of 9.01.

Bioinformatics and Phylogeny Analysis

To predict the functional characteristics of the novel protein in silico, we translated the nucleotide coding sequence in all three reading frames. The original BLASTX search (Altschul et al. 1997; Schäffer et al. 2001) indicated that only a single translated protein sequence (score, 587; e-value, 3×10^{-66}) gave consistent search results with the corresponding nucleotide sequence. The novel sequence showed a high level of sequence similarity to several prokaryotic polyprenyl and isoprenyl diphosphate synthases over the entire nucleotide/protein coding region. The highest sequence similarity (58% sequence identity; e-value, $1\times e^{-98}$) of the novel protein was assigned to a putative polyprenyl diphosphate synthase of the bacterium *Tenacibaculum* sp. By contrast, the novel protein sequence showed a significantly lower level of sequence similarity (14–19% sequence identity) to eukaryotic prenyl diphosphate synthases.

The seven conserved domains (I–VII) of prenylsynthases could be allocated to the same relative locations within the coding sequence (Chen et al. 1994). The aspartate-rich motifs (domain II and VI) which are implicated in substrate binding and catalysis were both present (Ashby et al. 1992; Song and Poulter 1994; Ohnuma et al. 1998).

As the initial BLASTX search of the isolated nucleotide/protein sequence did not give definitive information about its functional properties, we applied a more detailed sequence analysis employing the conserved domain database hosted at NCBI. The primary search (data not shown) of the protein sequence against CDD (Marchler-Bauer et al. 2005) indicated that the protein was a head to tail *trans*-isoprenyl diphosphate synthase. This enzyme class is able to catalyze the head to tail condensation of an allylic diphosphate donor with IPP, resulting in an elongated isoprenyl diphosphate

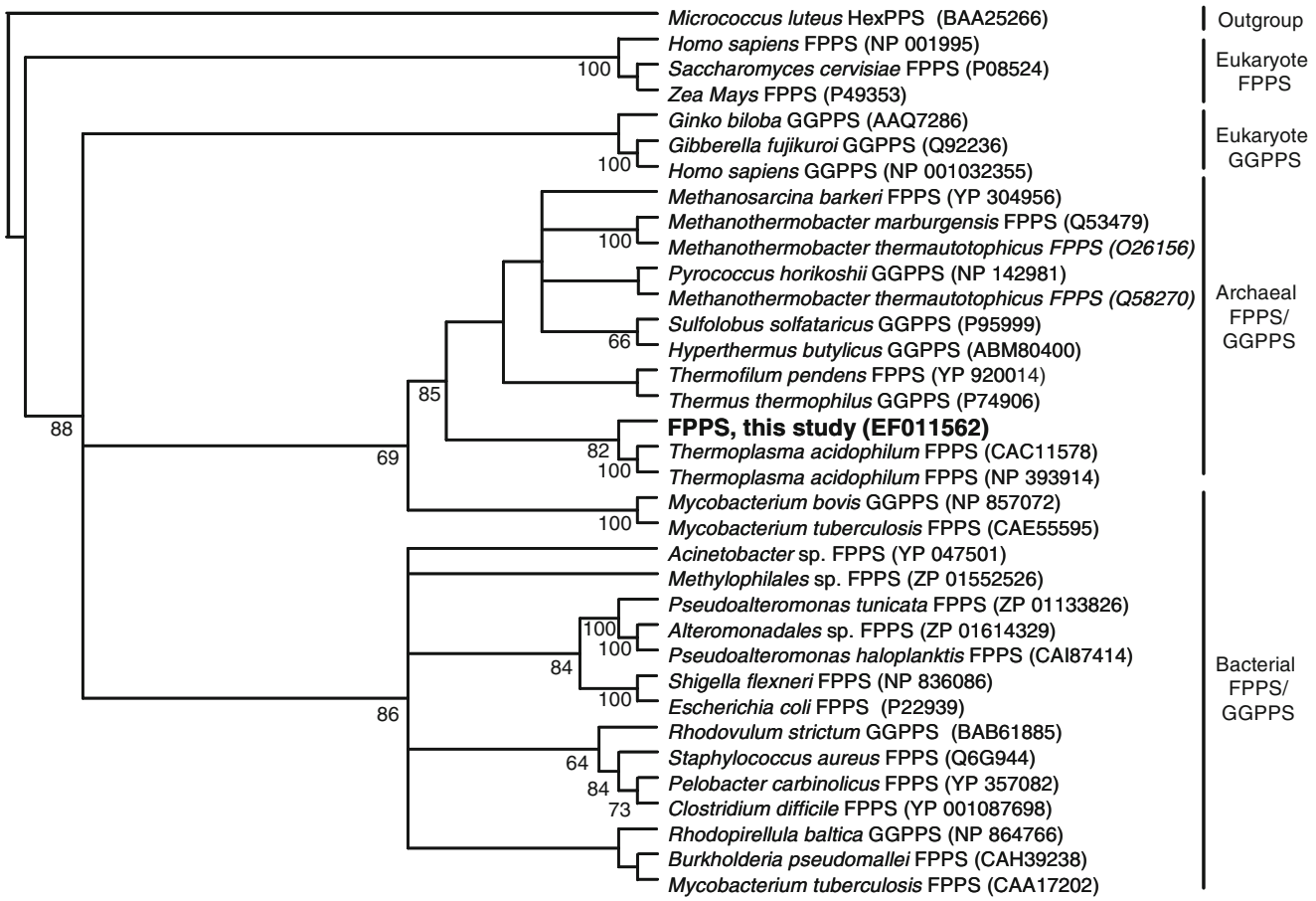

Fig. 2 Phylogeny of the novel FPPS sequence. The distance-based neighbor-joining algorithm was applied to all FPPS and GGPPS protein sequences. Bootstrap percentages after 1,000 replications for the most significantly supported clades are shown *below* the nodes. All sequences obtained from public databases are shown with their NCBI accession numbers in *parentheses*

with the *E*-configuration. A more refined analysis of the obtained protein sequence using the conserved DART (Geer et al. 2002) indicated that the catalytic domain of the novel protein resembled features of both GGPP and FPP synthases of prokaryotic origin (score, 963; e-value, 4×10^{-71}). Since the sequence similarity comparison could not definitively predict the evolutionary origin of the novel protein, we conducted a phylogenetic comparison using various prenyl diphosphate synthase sequences selected from NCBI's protein repository.

Figure 2 shows a distance phylogeny of the *E. fusca* derived *Symbiodinium* sp. farnesyldiphosphate synthase (FPPS) from this study, together with other FPPS and geranylgeranyl diphosphate synthase (GGPPS) sequences. All archaeal, bacterial, and eukaryotic FPP/GGPP synthase clusters grouped together with the exception of two mycobacterial FPPS/GGPPS sequences that seemed to be closely related to archaeal GGPP/FPP synthase sequences. The phylogenetic position of the FPP synthase sequence from this study strongly suggests its relatedness with archaeal GGPP/FPP synthases, being most closely affiliated to FPP synthase sequences from *Thermoplasma acidophilum* (Phylum: Euryarchaeota).

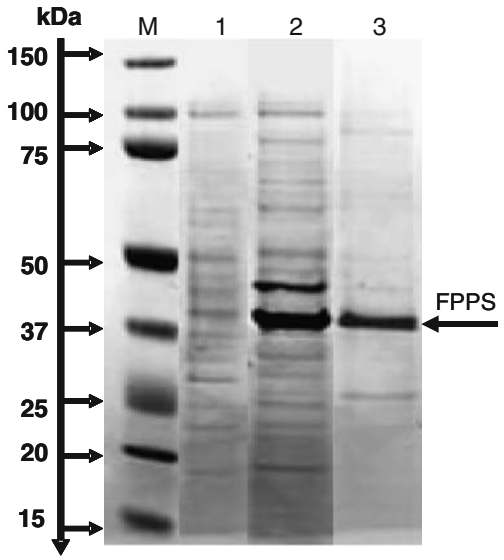

Fig. 3 SDS-PAGE (10% T) analysis of crude and purified recombinant FPPS expressed in *E. coli*. *Lane-M* Bio-Rad Precision Plus protein marker (12 μl), *1* crude *E. coli* cell lysate prior to IPTG induction (10 μg), *2* crude *E. coli* cell lysate after induction with 1 mM IPTG (13 μg), *3* recombinant FPPS fraction after Ni-affinity chromatography purification (8 μg). The recombinant FPPS is marked with an *arrow*

Heterologous Expression of EFZ265 in *E. Coli*

To definitively characterize the catalytic properties of the putative FPPS, we conducted a detailed kinetic study of the recombinant protein for prenylsynthase activity. We transformed the full-length gene, EFZ265, into the expression vector BL21 Star (DE3), which can be induced with IPTG to overexpress the introduced foreign gene. Transformation and induction resulted in a synthesized protein of the predicted molecular weight (Fig. 3), which was absent in the uninduced cell cohorts.

Product Identification Using Incubations of Cell Homogenates

Crude recombinant protein extracts of transformed *E. coli* were assayed for functional activity. Assays were performed using mixtures of IPP with either DMAPP, GPP, FPP, or GGPP as cosubstrates. Under the given reaction conditions, only the reaction of GPP with IPP lead to measurable product formation with FPP as the only product. The identity of the FPP formed during the reaction was confirmed by HPLC by co-injection with the authentic standard. These results were consistent with the bioinformatics data indicating that the enzyme is a *trans*-acting isoprenyl diphosphate synthase.

Enzyme Characterization

To elucidate the catalytic properties of the putative FPPS activity investigated in this study, we determined the substrate specificities and reaction velocities of this enzyme under steady state conditions using DMAPP, GPP, and FPP with the cosubstrate IPP. Additionally, we investigated the optimal pH and Mg^{2+} ion concentration required for catalysis. For the kinetic assays, the putative isoprenyl diphosphate synthase was purified from total protein extracts of transformed *E. coli* cells. The crude protein fraction was processed by Ni^{2+}-affinity FPLC eluting with 200 mM imidazole to afford the recombinant protein.

To evaluate the relative purity of the enzyme preparation obtained from the FPLC procedure, SDS-PAGE analysis of the respective protein fraction was performed. Examination of resulting protein patterns (see Fig. 3, lane 3) indicated that FPLC processing of the recombinant soluble protein fraction resulted in a approximately 95% purification and enrichment of a single protein species with an apparent molecular weight of approximately 38 kDa, which is in line with the calculated molecular weight. The purified enzyme fraction was evaluated for FPPS activity using our standard assay procedures; however, this resulted in relatively poor activities. Therefore, the assay buffer was modified by substituting various components used in the functional characterization of recombinant isoprenyl diphosphate synthases described in the literature (Ding et al. 1991; Dhiman et al. 2004). It was apparent that the addition of orthovanadate and the presence of the detergents Tween 20 as well as Triton X-100 resulted in a significant increase in enzyme activity (~7 fold) and stability (~2 fold).

A steady-state approach was employed to assess the reaction kinetics of the putative *E. fusca* derived isoprenyl

Table 2 Kinetic analysis of recombinant FPPS reaction with allylic substrates and variable Mg^{2+} concentration

Variable substrate	Measured product	R^2 of fit in (%)	K_m (μM)	V_{max} (pmol/min/μg protein)	k_{cat} (min^{-1})	k_{cat}/K_m ($min^{-1}M^{-1}$)
DMAPP	GOH	98	245±32	0.47±0.11	0.18	7.2×10^{2}
GPP	FOH	99	16±2	3.7±0.08	1.4	8.9×10^{4}
IPP	FOH	99	51±9	5.67±0.03	2.18	4.2×10^{4}
FPP	GGOH	98	58±7	$0.013\pm5\times10^{-3}$	4.94×10^{-3}	8.4×10^{1}
Mg^{2+}	FOH	99	3.7	6.25±0.04	2.4	6.35×10^{5}

diphosphate synthase. To study the reactions of different allylic substrates, we used varying concentrations (0–1,000 μM) of DMAPP, GPP, and FPP and a constant concentration of radiolabeled IPP as a cosubstrate. Conversely, when the reaction kinetics of the cosubstrate were examined, the concentration of radiolabeled IPP was varied, while a constant concentration of unlabeled GPP was supplied to the reaction mixture. The resulting isoprenyl diphosphate reaction products were subsequently converted to the corresponding alcohols (GOH, FOH, or GGOH) to generate a stable derivative for analysis. Therefore, reaction velocities for each substrate were expressed as the amount (picomole) of isoprenylalcohol produced per minute per microgram of enzyme. The plots of the reaction velocities versus substrate concentration (0–1,000 μM) displayed typical hyperbolic saturation curves (data not shown), which were fitted to the Michaelis–Menton equation, yielding the kinetic constants that are summarized in Table 2. The data suggests that both GPP and IPP are the preferred substrates of the enzyme with FPP as the final reaction product.

FPPS type enzymes commonly require Mg^{2+} or an alternative divalent metal (Chen and Poulter 1993) co-factor for catalytic activity. As these metal co-factors are thought to be involved in substrate binding, we have investigated the effect of Mg^{2+} concentration on the catalytic efficiency of the FPPS derived from *E. fusca*. The enzyme was completely inactive in metal-ion free assay buffer (see Fig. 4) and when 100 mM EDTA was added to the standard $MgCl_2$ containing buffer mixture used in kinetic experiments. Addition of Mg^{2+} ions restored the enzyme activity in a concentration dependent manner, as shown in Fig. 4. Increasing concentrations of Mg^{2+} resulted in a proportional increase of enzyme activity up to a maximal value of 6.25 pmol/min/μg protein at around 10 mM. The reaction kinetics for Mg^{2+} dependency showed typical saturation behavior and, therefore, kinetic constants were calculated using the Michaelis–Menton equation. The kinetic constants for Mg^{2+} dependency of the *E. fusca* derived FPPS are summarized in Table 2.

The optimal pH range for the FPPS was assessed using GPP and IPP as substrates (see Fig. 5). The enzyme was active over a relatively broad pH range (6.5–8.5), with an apparent optimal activity of 4.32 pmol/min/μg of enzyme at pH 7.5.

Discussion

The DD-PCR-based screening revealed many differentially expressed bands that corresponded to the trend found in the fuscol induction with SA (Fig. 1). One such band (cloned as EFZ265) represented a PCR product containing two DDXXD motifs which was approximately 450 bp long and was obtained using a degenerate upstream primer based on the conserved aspartate-rich domains of prenylsynthases. This PCR-generated fragment showed high sequence simi-

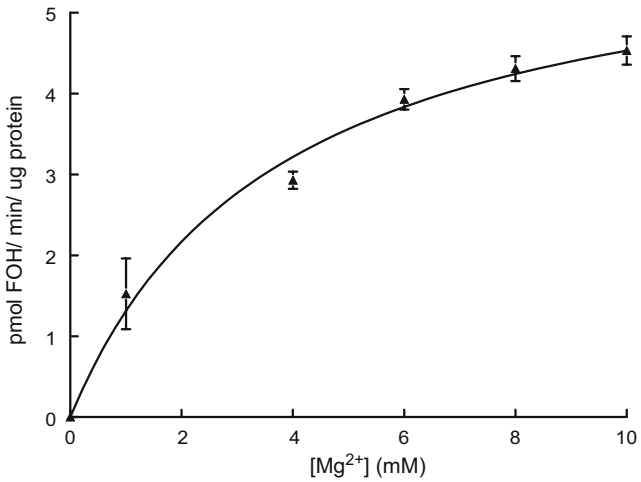

Fig. 4 Mg^{2+} requirement for FPPS activity

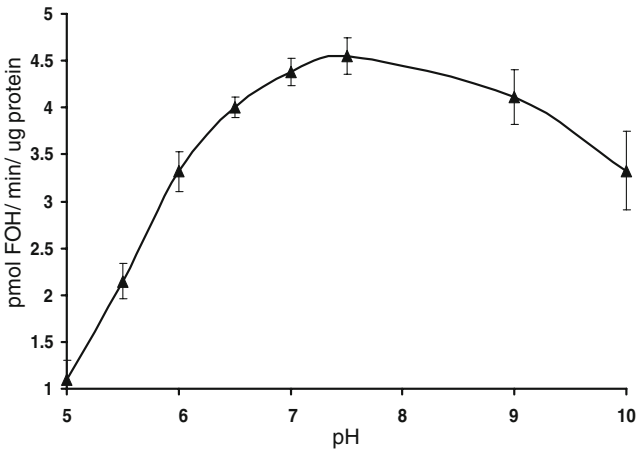

Fig. 5 pH dependence on FPPS activity

larity to known prenylsynthases. Several strategies were explored for the extension of this partial gene that appeared to be involved in terpene biosynthesis. Inverse PCR was used for the recovery of the regions flanking the known partial sequence. Additionally, the single-primer PCR method was employed and both methods led to the recovery of the full gene.

Evidence strongly suggests that the polypeptide encoded by the cloned cDNA catalyzed the formation of FPP from GPP and IPP, thus, encoding a FPPS. Such biosynthetic enzymes from terrestrial organisms have received a significant amount of attention. An FPPS was the first discovered in 1958 (Lynen et al. 1958, 1959) and these have now become the most widely occurring and best characterized prenylsynthases. FPPSs are either monomeric or homodimeric enzymes with subunits ranging in size from 32–44 kDa (Szkopinska and Plochocka 2005). The FPPS isolated in this study has an observed molecular weight of approximately 38 KDa, which is consistent with the molecular weight of other FPPSs of eukaryotic and microbial origin (Marrero et al. 1992; Tachibana et al. 2000).

Significant protein sequence similarity was observed between the FPPS isolated in this study and archaeal isoprenyl diphosphate synthases using standard phylogenetic alignment methods. Domain sequence analysis of the putative FPPS indicated several signature motifs common to many isoprenyl diphosphate synthases. Comparison of domains II and VI showed the presence of the putative substrate binding FARM and SARM signature sequences, respectively. Both the FARM and SARM domain each contain a canonical Asp rich (DDXXD or DDXXXXD) motif, which is thought to be responsible for substrate binding. Literature data suggests that all of the Asp residues in the FARM domain are important for binding of allylic substrates, while only the first two Asp residue in the SARM domain are critical for binding IPP (Wang and Ohnuma 2000; Szkopinska and Plochocka 2005). Besides the Asp residues in FARM and SARM domains, several lysine residues many also serve this function and indeed are known to be important in a number of enzyme actions of phosphorylated substrates (Riordan et al. 1977; Xia and Storm 1990; Carattoli et al. 1991).

To further characterize the catalytic properties of the *E. fusca* derived enzyme, we conducted a steady state kinetic analysis with various allylic substrates. The results summarized in Table 2 indicate that of the potential allylic substrates, DMAPP, GPP, and FPP tested in this study, only GPP served as a productive substrate of the enzyme resulting in FPP as the final product.

The K_m values and pseudo-second order rate constants (specificity constants) obtained in this study for both GPP and IPP compare favorably with those determined for the FPPS from *Mycobacterium tuberculosis* (Dhiman et al. 2004) and other eubacteria (Takahashi and Ogura 1981; Kawasaki et al. 2003). In contrast, the determined kinetic parameters differ from those of eukaryotic enzymes, such as human FPPS (Ding et al. 1991), rat liver FPPS (Marrero et al. 1992), and the FPPS FDS-1 of the plant *Artemisia tridentate* (Hermmerlin et al. 2003).

Many FPPSs effectively synthesize FPP from either DMAPP or GPP as allylic substrates (Reed and Rilling 1976; Koyama et al. 1977; Green and West 1974). If FPP is synthesized from IPP and DMAPP by a single enzyme, two condensations of IPP with the allylic substrate are catalyzed, releasing only small amounts of GPP as the intermediate (Ishii et al. 1986). The conversion of DMAPP and IPP with the *E. fusca*-derived FPPS investigated in this study did not result in significant levels of GPP or FPP as reaction products under the given reaction conditions (see Table 2). The affinity of the enzyme for DMAPP as the allylic substrate was approximately 20 times lower than the equivalent reaction with GPP as reflected in the respective K_m values (Table 2). Similarly, comparison of the respective specificity constants (k_{cat}/K_m) indicated a 100 times higher specificity for GPP compared to DMAPP as the allylic substrate.

While many eukaryotic and bacterial FPPSs are capable of synthesizing FPP from both DMAPP and IPP as the starting substrates, recent literature suggests that GPP and not DMAPP may serve as the favored allylic substrate (Szkopinska and Plochocka 2005). One prominent example is the farnesyl diphosphate synthase of the rubber producing fungus *Lactarius chrysorrheus*, which utilizes GPP as the primary substrate with a 2.4 fold higher pseudo-first order rate (k_{cat}/K_m) constant compared to the equivalent reaction with DMAPP (Mekkriengkrai et al. 2004). Similarly, preferential utilization of GPP versus DMAPP as the allylic substrate for FPP synthesis has been observed in cell culture experiments with the Californian poppy plant (*Escholzia californica*; Roos et al. 1998). Analogous to the substrate preference observed in this study, both the ω,*E,E*- and ω,*E,Z*-FPPS from *M. tuberculosis* exclusively accept GPP as the allylic reaction partner for IPP condensation (Dhiman et al. 2004).

With the exception of some bifunctional FPPS/GGPPS enzymes of archaeal origin (Tachibana et al. 2000), designated FPPSs do not undergo a productive interaction with IPP, when either FPP or GGPP are supplied as allylic substrates (Wang and Ohnuma 2000). This literature data is consistent with the results of our product analysis and the kinetic parameters determined for the reaction of FPP and IPP with the FPPS derived from *E. fusca*. As expected, the catalytic rate constant (k_{cat}) for FPP as the allylic substrate was approximately 1,000 times smaller than the equivalent rate constants for either GPP or IPP (Table 2). Interestingly, the affinity for FPP as a substrate was comparable to that of IPP as inferred from the respective K_m values. Therefore, FPP may actually bind to enzyme's active site (FARM motif) but its productive interaction with the cosubstrate IPP may be disturbed due to steric constraints. Alternatively, FPP may

react with IPP effectively but the bulky reaction product GGPP may not be released from the active site. Indeed, in addition to the initial rate of carbocation formation, the rate of product release from the active site is a main contributor to observed k_{cat} values of isoprenyl diphosphate synthases (Wang and Ohnuma 2000).

It is now commonly accepted that isoprenyl diphosphate synthase selectivity is regulated by the amino acid residues located at the fourth and fifth positions N-terminal to the FARM motif at the bottom of the active site pocket. Hence, this particular signature sequence is termed the chain-length determining (CLD) region. It is thought that the amino acids of the CLD region exert their effect on product selectivity through direct steric and electrostatic interactions with the ω-terminal region of the allylic substrates (Szkopinska and Plochocka 2005). Protein sequence analysis of the isoprenyl diphosphate synthase examined in this study showed that the amino acid residues placed at the fourth and fifth position of the CLD region constitute Ala and Thr, respectively. This particular arrangement of amino acid residues, however, resembles the CLD region of bacterial GGPPSs and higher isoprenyl diphosphate synthases but not FPPSs, which generally have at least one aromatic amino acid residue, such as Phe, Tyr, or Trp either at the fourth or fifth position N-terminal to the FARM region (Wang and Ohnuma 2000). Therefore, based on sequence analysis, it was expected that the *E. fusca* derived isoprenyl diphosphate synthase in this study showed product selectivities typical of GGPPSs and not FPPSs. However, in slight contrast to the results of the sequence analysis, both product analysis and kinetic examination clearly indicated that the enzyme showed selective production of FPP and not GGPP (or higher isoprenyl diphosphates). A discordance between the results of classical signature sequence and actual product analysis has also been reported for the ω, *E,E*-farnesyldiphosphate synthase of *M. tuberculosis* (Dhiman et al. 2004). This particular enzyme showed the typical arrangements of amino acid in the catalytic FARM domain and the CLD region, which are characteristic of archaeal (type I) GGPPSs; however, a detailed product analysis and kinetic study of the recombinant enzyme indicated selective FPPS activity. Since the signature sequences, product analysis, and kinetic parameters for the enzyme examined in this study closely resemble those of the FPPS from *M. tuberculosis*, structural features other than the established amino acid assemblies within the FARM and CLD domains may contribute to the catalytic activities and product selectivities of particular short-chain isoprenyl diphosphate synthases.

The optimal pH activity range (pH 6–8) of the *E. fusca*-derived enzyme was in close agreement with data for a variety of other farnesyldiphosphate synthases (Schulbach et al. 2001; Hermmerlin et al. 2003; Dhiman et al. 2004). Much like the pH profile of the enzyme, the optimal Mg^{2+} concentration and saturation behavior was in accord with existing literature for FPPSs (Schulbach et al. 2001; Kawasaki et al. 2003; Dhiman et al. 2004; Szkopinska and Plochocka 2005). This close agreement of the literature data for optimal pH ranges and Mg^{2+} concentrations of FPPSs from different phyla indicates that these factors stringently control enzyme activity.

The kinetic data and product specificity determined for this FPPS is very similar with reported data for eubacterial and archaeal FPPSs. However, the phylogenetic position of the *E. fusca*-/*Symbiodinium* sp.-derived FPPS found in this study was noticeably within the archaeal FPP/GGPP synthase group, specifically clustering with two euryarchaeotal FPPS sequences. Since euryarchaeotal FPP synthases have not been thoroughly studied, direct reference to their catalytic properties cannot be made at this time.

The data suggests that the archaeal-like FPPS examined in this study may have either been introduced into the dinoflagellate genome by horizontal gene transfer (Lawrence and Roth 1996) or it originated from a prokaryotic source organism associated with the dinoflagellate symbionts of *E. fusca*. This latter option is consistent with observations that octocoral such as *E. fusca* and their respective dinoflagellate symbionts are host to specific microbial assemblies (Brück et al. 2007; Rosenberg et al. 2007; Sapp et al. 2007). While a possible or likely association between coral and archaea has been demonstrated in several studies, the interaction between these organisms and its biological significance still remains to be established (Rosenberg et al. 2007). There have been few reports about prokaryotic isoprenoid synthases/cyclases genes as the vast majority of isoprenoids are produced by eukaryotes Bohlmann et al. 1998; Kleemann et al. 1994; Reipen et al. 1995; Wendt et al. 1997). This is the first description of a prokaryotic FPPS isolated from the metagenome of a marine invertebrate. In summary, we present a DD-PCR-based approach that led to the isolation of a prenyl diphosphate that was transcriptionally activated under conditions that led to an induction of fuscol biosynthesis.

Acknowledgements The authors gratefully acknowledge financial support from Florida Sea Grant (R/LR-MB-14), the Center of Excellence in Biomedical and Marine Biotechnology, the University of Prince Edward Island, the Canada Research Chair program, and the J.L. Lévesque Foundation. We would also like to thank Dr. Stefan W. Vetter (Florida Atlantic University) for his assistance with protein expression.

References

Altschul SF, Madden TL, Schäffer AA, Zhang J, Zhang Z, Miller W, Lipman DJ (1997) Gapped BLAST and PSI-BLAST: a new generation of protein database search programs. Nucleic Acids Res 25:3389–3402

Ashby MN, Kutsunai SY, Ackerman S, Tzagoloff A, Edwards PA (1992) COQ2 is a candidate for the structural gene encoding parahydroxybenzoate: polyprenyl-synthase. J Biol Chem 267:4128–4136

Bohlmann J, Meyer-Gauen G, Croteau R (1998) Plant terpenoid synthases: molecular biology and phylogenetic analysis. Proc Natl Acad Sci U S A 95:4126–4133

Bradford MM (1976) A rapid and sensitive method for the quantitation of microgram quantities of protein utilizing the principle of protein-dye binding. Anal Biochem 72:248–254

Brück TB, Brück WM, Santiago-Vazquez LZ, McCarthy PJ, Kerr RG (2007) Diversity of bacterial communities associated with Azooxanthellate deep water *octocorals Leptogorgia minimata, Iciligorgia schrammi, Swiftia exertia*. Mar Biotechnol 9(5):561–576 (ahead of print)

Carattoli A, Romano N, Ballario P, Morelli G, Macino G (1991) The *Neurospora crassa* carotenoids biosynthetic gene (albino 3) reveals highly conserved regions among prenylsynthases. J Bio Chem 266(9):5854–5859

Chen A, Poulter CD (1993) Purification and characterization of farnesyl/geranygeranyl diphosphate synthase. A thermostable bifunctional enzyme from *Methanobacterium thermoautotrophicum*. J Biol Chem 268(15):1102–1107

Chen A, Kroon PA, Poulter CD (1994) Isoprenyl diphosphate synthases: protein sequence comparisons, a phylogenetic tree, and prediction of secondary structure. Protein Sci 3:600–607

Dhiman RK, Schulbach MC, Mahapatra S, Baulard AR, Vissa V, Brennan PJ, Crick DC (2004) Identification of a novel class of ω, E, E,-farnesyldiphosphate synthase from *Mycobacterium tuberculosis*. J Lipid Res 45:1140–1147

Ding VD, Shears BT, Bergstrom JD, Ponpipom MM, Perez LB, Poulters CD (1991) Purification and characterization of recombinant human farnesyldiphosphate synthase expressed in *E. coli*. Biochem J 275 (Pt 1):61–65

Geer MY, Domrachev M, Lipman D, Ryant S (2002) CDART: protein homology by domain architecture. Genome Res 12:1619–1623

Gershenzon J, Croteau R (1993) In: Moore TS Jr (ed) Lipid metabolism in plants. CRC, Boca Raton, FL, pp 339–388

Green TR, West CA (1974) Purification and characterization of 2 forms of geranyl synthase from *Ricinus communis*. Biochemistry 13:4720–4729

Hampel D, Mosandl A, Wüst M (2005) Induced biosynthesis of terpenoids in *Vitis vinifera* L.: crosstalk between cytosolic MVA- and plastidial DOXP/MEP-pathway. J Agric Food Chem 53(7):2652–2657

Hermmerlin A, Rivera SB, Erickson HK, Poulter CD (2003) Enzymes encoded by the farnesyl diphosphate synthase gene family in the big sagebrush *Aretisima tridentata ssp. Spiciformis*. J Biol Chem 278(34):32132–32140

Ishii K, Sagami H, Ogura K (1986) A novel prenyltransferase from Paracoccus denitrificans. Biochem J 233:773–777

Kawasaki T, Hamano Y, Kuzuyama T, Itoh N, Seto H, Dairi T (2003) Interconversion of the product specificity of type I eubacterial farnesyl diphosphate synthase and geranylgeranyl diphosphate synthase through one amino acid substitution. J Biochem (Tokyo) 133(1):83–91

Kleemann G, Kellner R, Poralla K (1994) Purification and properties of the squalene–hopene cyclases from *Rhodoseudomonas palustris*, a purple non-sulfur bacterium producing hopanoids and tetrahymanol. Biochim Biophys Acta 1210:317–320

Koyama T, Saito Y, Ogura K, Seto S (1977) 2 forms of farnesylpyrophosphate synthase from hog liver. J Biochem (Tokyo) 82:1585–1590

Koyama T, Obata S, Osage M, Takeshita A, Yokoyama K, Uchida M, Nishino T, Ogura K (1993) Thermostable farnesyl diphosphate synthase of *Bacillus stearothermophylus*: molecular cloning, sequence determination, overproduction and purification. J Biochem 113:355–363

Laing P, Pardee AB (1992) Differential display of eukaryotic messenger RNA by means of the polymerase chain reaction. Science 257:967–971

Lammlie UK (1970) Cleavage of structural proteins during the assembly of the head of bacteriophage T4. Nature 227:680–685

Lawrence JG, Roth JR (1996) Selfish operons: horizontal transfer may drive the evolution of gene clusters. Genetics 143:1843–1860

Lynen F, Efferer H, Henning U, Kessel I (1958) Farnesyl-pyrophosphat und 3-methyl-Δ3-butenyl-1-pyrophosphat, die biologischen vorstufen des squalens. Zur biosynthase der terpene, III. Angew Chem 70:738–742

Lynen F, Agranoff BW, Eggerer H, Henning U, Moslein EM (1959) γ-Dimethylallylpyrophosphat und geranyl-pyrophosphat, biologische vorstufen des squalens. Zur biosynthese der terpene VI. Ange Chem 71:657–663

Marchler-Bauer A, Anderson JB, Cherukuri PF, DeWeese-Scott C, Geer LY, Gwadz M, He S, Hurwitz DI, Jackson JD, Ke Z, Lanczycki CJ, Liebert CA, Liu C, Lu F, Marchler GH, Mullokandov M, Shoemaker BA, Simonyan V, Song JS, Thiessen PA, Yamashita RA, Yin JJ, Zhang D, Bryant SH (2005) CDD: a conserved domain database for protein classification. Nucleic Acids Res 33:D192–D196

Marrero PF, Poulter CD, Edwards PA (1992) Effects of site-directed mutagenesis of the highly conserved aspirate residues in domain II of farnesyl diphosphate synthase activity. J Biol Chem 267 (30):21873–2178

Mekkriengkrai D, Sando T, Hirooka K, Sakdapipanich J, Tanaka Y, Fukusaki E, Kobayashi A (2004) Cloning and characterization of farnesyl diphosphate synthase from the rubber-producing mushroom *Lactaris chrysorrheus*. Biosci Biotechnol Biochem 68: 2360–2368

Newberger NC, Ranzer LK, Boehnlein JM, Kerr RG (2006) Induction of terpene biosynthesis in dinoflagellate symbionts of Caribbean gorgonians. Phytochemistry 67(19):2133–2139

Ohnuma S, Hirooka K, Tsuruoka N, Yano M, Ohto C, Nakane H, Nishino T (1998) A pathway where polyprenyl diphosphate elongates in prenylsynthases. Insight into a common mechanism of chain length determination of prenylsynthases. J Biol Chem 273:26705–26713

Reed BC, Rilling HC (1976) Substrate binding of avian liver prenylsynthase. Biochemistry 15:3739–3745

Reipen IG, Poralla K, Sahm H, Sprenger GA (1995) *Zymomonas mobilis* squalene-hopene cyclase gene (shc): cloning, DNA sequence analysis, and expression in *Escherichia coli*. Microbiology 141:155–161

Riordan JF, McElvany KD, Borders CL Jr (1977) Arginyl residues and anion binding sites in enzymes. Science 195:884–886

Roos W, Evers S, Hieke M, Tschope M (1998) Shifts of intracellulare pH distribution as part of the signal mechanism leading to the elicidation of benzophenanthridine alkaloids in *Eschscholtzia californics*. Plant Physiol 118:349–364

Rosenberg E, Koren O, Reshef L, Efrony R, Zilber-Rosenberg I (2007) The role of microorganisms in coral health, disease and evolution. Nat Rev Microbiol 5(5):355–362

Sapp M, Schwaderer AS, Wiltshire KH, Hoppe HG, Gerdts G, Wichels A (2007) Species-specific bacterial communities in the phycosphere of microalgae? Microb Ecol 53(4):683–699

Schäffer AA, Aravind L, Madden TL, Shavirin S, Spouge JL, Wolf YI, Koonin EV, Altschul SF (2001) Improving the accuracy of PSI-BLAST protein database searches with composition-based statistics and other refinements. Nucleic Acids Res 29:2994–3005

Schulbach MC, Mhahapatra S, Maccia M, Barontini S, Papi C, Minutolo F, Bertini S, Brennan PJ, Crick DC (2001) Purification, enzymatic characterization, and inhibition of the Z-farnesyldiphosphate synthase from *Mycobacterium tuberculosis*. J Biol Chem 276(15):11624–11630

Sembdner G, Parthier B (1993) Biosynthesis and action of jasmonates in plants. Annu Rev Plant Physiol Plant Mol Biol 44:569–589

Shulaev V, Silverman P, Raskin I (1997) Airborne signalling by methyl salicylate in plant pathogen resistance. Nature 385:718–721

Song L, Poulter CD (1994) Yeast farnesyl-diphosphate synthase: site-directed mutagenesis of residues in highly conserved prenylsynthases domains I and II. Proc Natl Acad Sci U S A 91:3044–3048

Stanley-Fernandez SM, Kellog BA, Poulter CD (2000) Farnesyl diphosphate synthase, altering the catalytic site to select for geranyldiphosphate activity. Biochem 39:15316–15321

Swofforf DL (2001) PAUP: phylogenetic analysis using parsimony. Version 4.0b8. [Online] http://paup.csit.fsu.edu/index.html. Sinauer Associates, Sunderland, Massachusetts

Szkopinska A, Plochocka D (2005) Farnesyl diphosphate synthase regulation of product formation. Acta Biochim Polonika 52(1): 45–55

Tachibana A, Yano Y, Otani S, Nomura N, Sako Y, Taniguchi M (2000) Novel prenylsynthase gene encoding farnesylgeranyl diphosphate synthase from the hyperthermophilic archaeon, *Aeropyrum pernix*. Molecular evolution with alteration in product specificity. Eur J Biochem 267:321–328

Takahashi I, Ogura K (1981) Farnesyl pyrophosphate synthetase from *Bacillus subtilis*. J Biochem (Tokyo) 89(5):1581–1587

Takaya A, Zhang YW, Asawatreratanakul K, Wititsuwannakul D, Wititsuwannakul R, Takahashi S, Koyama T (2003) Cloning, expression and characterization of a functional cDNA clone encoding geranylgeranyl diphosphate synthase of *Hevea brasilliensis*. Biochim Biophs Acta 1625:214–220

Thompson JD, Gibson TJ, Plewniak F, Jeanmougin F, Higgins DG (1997) The CLUSTAL_X windows interface: flexible strategies for multiple sequence alignment aided by quality analysis tools. Nucleic Acids Res 25:4876–4882

Wang K, Ohnuma S (2000) Isoprenyl diphosphate synthases. Biochim Biophys Acta 1529:33–48

Wendt K, Poralla K, Schulz GE (1997) Structure and function of a squalene cyclase. Science 277:1811–1815

Wiedemann M, Misawa N, Sandmann G (1993) Purification and enzymatic characterization of the geranygeranyl pyrophosphate synthase from *Erinia uredovora* after exresssion in *E.coli*. Arch Biochem Biophys 306:152–157

Xia ZG, Storm DR (1990) A-type ATP binding consensus sequences are critical for the catalytic activity of the calmodulin-sensitive adenylyl cyclase from *Bacillus anthracis*. J Biol Chem 265:517–6520

Zhang D, Poulter CD (1993) Analysis and purification of phosphorylated isoprenoids by reversed-phase HPLC. Anal Biochem 213: 356–361